Available online at www.sciencedirect.com
ScienceDirect
International Journal of Mass Spectrometry 266 (2007) 156–165
International Journal of Mass Spectrometry
www.elsevier.com/locate/ijms

Comparison of ion trajectories in vacuum and viscous environments using SIMION: Insights for instrument design

David A. Dahl [1], Timothy R. McJunkin, Jill R. Scott *

Chemical Sciences, Idaho National Laboratory, Idaho Falls, ID 83404, United States

Received 16 May 2007; accepted 18 July 2007
Available online 22 July 2007

Abstract

The effective use of electrostatic and magnetic fields to control ion motion serves as the foundation for many scientific instruments. The advent of powerful personal computers and simulation programs, such as SIMION, have served to broaden the understanding of ion motion in vacuum throughout the scientific instrument community. The relatively recent development of a statistical dynamics simulation user program for SIMION 7.0 has provided a more accessible view into ion motions at elevated pressures and the opportunity to more fully illuminate ion motion differences between vacuum and viscous environments (e.g., electrostatic refraction, motion through grids, and magnetic fields). The loss of kinetic energy limits options for controlling ion motion in viscous conditions. For refraction, only net accelerating field methods (converging or diverging) are possible in viscous regimes. Motion of ions around wires in grids also has more severe consequences in viscous conditions than in vacuum. For magnetic fields, a good "rule-of-thumb" is that an ion must be able to complete a significant fraction of its cyclotron radius between collisions for the magnetic field to affect ion diffusion. At slightly reduced pressures, combined magnetic and electrostatic fields can be used to control ion trajectories. The difference in ion behavior is governed by the fact that kinetic energy of ion motion is retained in vacuum, but lost to collisions with the bath gas in viscous atmospheres. Because of the loss of kinetic energy, ion behavior in electrostatic and magnetic fields under viscous conditions is dramatically different than in vacuum.
Published by Elsevier B.V.

Keywords: Ion motion; Vacuum; Atmosphere; Spectrometry; Simulation

1. Introduction

Understanding how ions behave in electrostatic and magnetic fields is essential for design and understanding of scientific instruments that function in vacuum and/or viscous environments. Prior to the advent of effective methods of simulation, scientific instruments were frequently designed using an empirical, trial-and-error approach. However, high performance personal computers using modern simulation software, such as the SIMION 3D program, can simulate ion trajectories for a wide range of electrostatic and/or magnetic fields arrangements in vacuum conditions [1]. Specifically, SIMION 3D for the PC [2,3] has made a significant contribution to the field of mass spectrometry (MS) [4] because it enabled not only individual components [5–13], but also complete instruments to be designed and optimized prior to fabrication [14–19], essentially creating realistic virtual instruments [20]. This simulation capability in vacuum has helped foster a host of new mass spectrometer designs as well as other instrumentation [21–25], such as ion gauges [26]. Simulation software for ion motion in viscous atmospheres within electrostatic fields has been consigned to molecular dynamics simulations [27,28], which have not matured to the point of modeling complete instruments. Therefore, development of viscous atmosphere devices, such as ion mobility spectrometry (IMS) instruments, still depend on empirical approaches for many aspects of their designs, with the exception that simulation software programs have been used to design electrostatic potential gradients [29,30]. However, rapid simulation of how groups of ions will generally behave in those electrostatic fields at atmospheric pressure has been difficult until the introduction of the statistical diffusion simulation (SDS) user program for SIMION [31].

* Corresponding author at: Chemical Sciences, Idaho National Laboratory, 2525 N. Fremont Avenue, Idaho Falls, ID 83415, United States.
Tel.: +1 208 526 0429; fax: +1 208 526 8541.
E-mail address: jill.scott@inl.gov (J.R. Scott).
[1] Retired.

1387-3806/$ – see front matter. Published by Elsevier B.V.
doi:10.1016/j.ijms.2007.07.008

The modeling approach uses the well-established SIMION 7.0 program to simulate ion motion in vacuum and a combination of SIMION in conjunction with the SDS user program for ion motion in viscous media. The SDS user program for SIMION treats viscous drift motions and diffusion as two separate phenomena, although in reality they are not independent. A relatively straightforward viscous motion model is used to simulate viscous effects. Diffusion presents a more challenging problem because the millions of collisions per second that cause diffusion are very complex and time consuming to simulate stochastically. To speed up the calculations, SDS makes use of a collection of tabulated collision statistics with randomized ion jumping to provide a relatively unbiased estimate of diffusion through a wide range of ratios of ion to bath gas masses. The unbiased nature of the estimate is maintained so long as the number of collisions between time steps is sufficient to decorrelate the ion's successive velocity vectors [31].

Simulations using the SIMION/SDS approach can provide useful insights, perspectives, and understanding of issues and solutions for ion motion in viscous regimes. The applicability of this approach to atmospheric instruments, such as IMS, should be excellent so long as the ion velocity induced by the instrument is a small fraction of the ion's thermal velocity. This assumption should be true for IMS, as illustrated by examining cesium ions (Cs^+) drifting in an 8-in. long linear IMS with a 20 kV voltage drop (100 V/mm gradient) at standard atmospheric conditions. The thermal velocity of the Cs^+ ions at standard room temperature and pressure is approximately 220 m/s [32,33]. The IMS drift velocity of the cesium ions would be approximately 17 m/s or about 8% of the thermal velocity under these conditions. Most IMS applications use gradients 20 times less than that used in the example; therefore, for practical IMS instruments, arcing of electrostatic voltages would probably become a problem long before simulation accuracy. One caveat is that rigorous examination of the accuracy falloff as a function of pressure has yet to be performed for the SIMION/SDS modeling approach; however, the simulations are consistent with experimental evidence [31].

Comparison of ion motion in vacuum with that in a viscous media using SIMION with and without SDS is used to provide insights into the different behavior of ions concerning electrostatic refraction, influence of wire grids, and magnetic fields. These results illustrate that intuition about ion motion in vacuum can actually be a hindrance to designing instruments operating in viscous environments because the rules governing ion motion in viscous media are quite different than those in vacuum.

2. Methods

2.1. Electrostatic field effects modeling

SIMION 7.0 for electrostatic field modeling was used as commercially available (SIS, Ringoes, NJ) for modeling the vacuum illustrations. The algorithms and simulation approach employed by SIMION have been described previously [2,3,34,35]. Incorporation of diffusion effects into the modeling was accomplished by combining the SDS user program with SIMION 7.0. The details of the SDS algorithms for mobility and diffusion and have been published previously along with experimental validation of the modeling accuracy [31]. Standard temperature (25 °C) and pressure (760 Torr) were used for the viscous media simulations. Ions were introduced from either point or line sources as stated for each illustration.

2.2. Magnetic field effects modeling

Two modeling approaches were used to illustrate effects of magnetic fields on ion motion. To use the basic SIMION/SDS combination, the SDS user program (SDS.PRG) was associated with the magnetic array (i.e., MAG.PA0 was created via copying SDS.PRG to a file called MAG.PRG). The electrostatic array then had no associated user program attached because SIMION 7.0 accumulates ion acceleration terms in a given order, such that any magnetic effects are accumulated last. Therefore, the user program must be associated with the magnetic array to ensure that the total ion acceleration is processed by the Stoke's law of viscosity (ion mobility) user program segment. This method was used to explore the combined effects of magnetic and electrostatic fields on ion trajectories. While SIMION/SDS also simulates the effect of magnetic fields on diffusion, a second approach was used to more easily create illustrations of the observed effects.

For illustrating the effects of magnetic fields on diffusion, a SIMION user program was developed that compares an ion's trajectory without a magnetic field with the same ion's trajectory with a magnetic field present at atmospheric pressure. Initially, the ion was flown with the magnetic field set to zero after the random number generator was reset. To simplify the collision calculations, the ion was only allowed to have 2D collisions (i.e., ions were only allowed to move in the x–y plane, where $z = 0$). Although contrived, a nitrogen molecular ion (N_2^+) with a mass-to-charge ratio (m/z) of 28 was flown in a bath gas of nitrogen (N_2, 28 u) to eliminate mass differences between the ion and the collision gas to simplify the illustrations. The nitrogen molecular ion was initialized to have an average thermal velocity at standard temperature (25 °C) and pressure (760 Torr) of 475 m/s [32,33]. Under these conditions, the expected mean time between collisions would be 1.4×10^{-10} s, which is equivalent to a mean free path of 6.7×10^{-8} m. After each collision, the ion was given back its average thermal velocity and a random direction from 0° to 360° in elevation (i.e., ion stays in the same x–y plane, where $z = 0$). To compare the motion of the ion without and with a magnetic field present, the random number generator was again reset prior to flying the ion with a magnetic field present; thus, both the trajectories should be identical if the magnetic field has no effect. Note that resetting the random number generator to compare the two trajectories is only possible during the same SIMION session (i.e., if the SIMION program is closed and reopened between simulations, then the random number generator will not be reset to the same value). For the second ion trajectory, the magnetic field was set to a value between 7 and 7000 T.

3. Results and discussion

3.1. Collision effects on ion trajectories

Ion behavior is completely different in viscous (atmospheric pressure) environments than in vacuum. In Fig. 1, three point sources of 101 ions each were flown down a constant electrostatic gradient, through an "ideal" grid (i.e., ions are exposed to the electrostatic field, but do not collide with wires of the grid, which is impossible in reality), and into a zero gradient (i.e., field-free) region. The ideal grid acts to separate the two electrostatic gradients without having any solid objects that might neutralize or "kill" the ions. In vacuum, ion velocity is governed by inertia, as demonstrated in Fig. 1a, where the ions accelerate in an electrostatic gradient. After reaching the grid, the ions in vacuum maintain their kinetic energy and drift at their terminal velocity through the field-free region; thus, an ion's inertia is retained in a vacuum in zero gradient electrostatic fields.

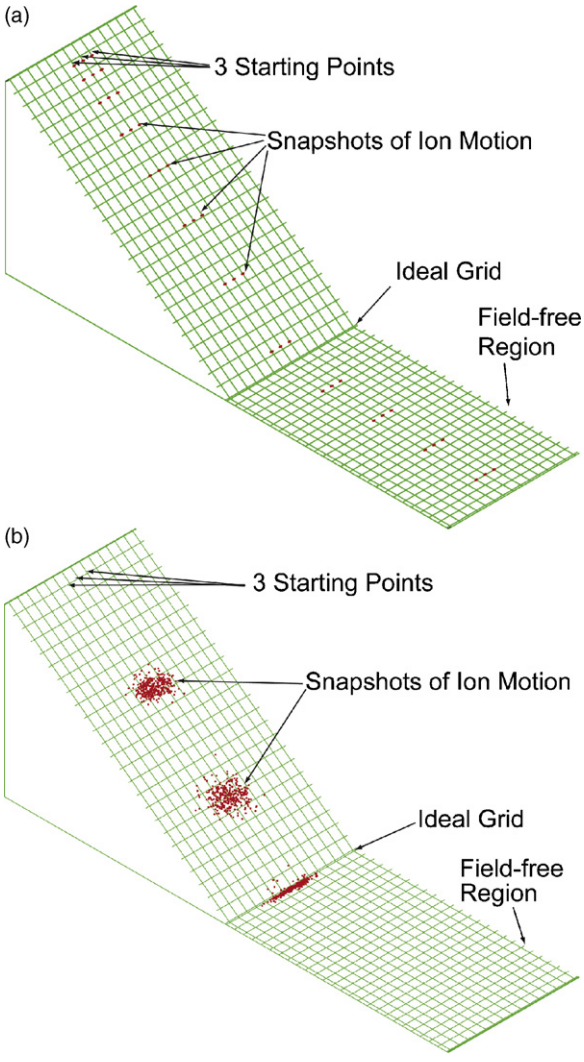

Fig. 1. Comparison of ion motion in (a) vacuum and (b) viscous environments showing snapshots of ion movement. Ions introduced at three starting points (101 ions at each point) and allowed to drift down an initial gradient, through an ideal grid, and into a field-free region.

However, ions in a viscous regime have no retained "inertia" as it relates to drift velocity because drift kinetic energy is lost almost immediately to gas collisions, as illustrated in Fig. 1b. In a viscous regime, ions gain energy from the electric field between collisions and lose energy to collisions; thus, ions rapidly attain a terminal drift velocity that is proportional to the electrostatic gradient, which is consistent with ion mobility theory [36]. The terminal drift velocity for a given ion type will be dependent on its effective collisional cross-section area. As shown in Fig. 1b, the ions in viscous media fly down the gradient at a constant drift velocity while diffusion causes the ion cloud to disperse. When the ions reach the ideal grid, they lose their drift velocity in the field-free region because the ion motion is overwhelmed by the number of collisions when no gradient is dragging the ions (i.e., the ions' terminal drift velocity is equal to zero). At this point, the ions slowly begin to diffuse into and would eventually be found throughout the field-free region. In general, if an electrostatic gradient is present, then an ion's drift trajectory will be down the gradient streamlines with an average velocity proportional to the local gradient in viscous media; however, if there is no voltage gradient in a viscous environment, there will be no ion drift velocity and ion motion will be induced only by diffusion.

This general difference in ion motion behavior is the reason that time-of-flight MS (i.e., vacuum) use a field-free region after accelerating the ions and IMS (i.e., viscous media) uses a drift region with an electrostatic gradient to keep the ions moving. The difference in retaining or not retaining kinetic energy, which is a direct result of collisions, has a profound affect on how ions can be controlled, as illustrated for electrostatic refraction, motion through grids, and magnetic fields.

3.2. Electrostatic refraction effects

Nonlinear gradient electrostatic fields are often used to focus or defocus beams of ions in vacuum where there are five types of refraction available. Refraction methods that involve a net increase or decrease in kinetic energy can be used for either converging or diverging lens designs in vacuum. Another converging only refraction type available in vacuum occurs with no net kinetic energy change (e.g., Enziel lens [10,37]). While all five approaches to ion refraction are available in vacuum and have been thoroughly exploited in mass spectrometer designs, only acceleration-based refraction (converging or diverging) is possible in viscous environments because of the loss of kinetic energy to collisions with the bath gas. Thus, refraction where kinetic energy is continually being pumped into the ions by an electrostatic gradient is the only viable refraction approach for viscous media. The results of accelerated converging and diverging refraction are significantly different for vacuum and viscous conditions.

Fig. 2 illustrates the trajectories of a line packet of 303 ions moving through a converging acceleration optics stage for vacuum (Fig. 2a) and viscous (Fig. 2b) environments. The voltage gradients for both environments are identical. In both examples, the ion packets focus or converge in the direction normal to their flight path. In the case of ions in vacuum (Fig. 2a), there is a small but noticeable loss of time focus (i.e., broadening of ion

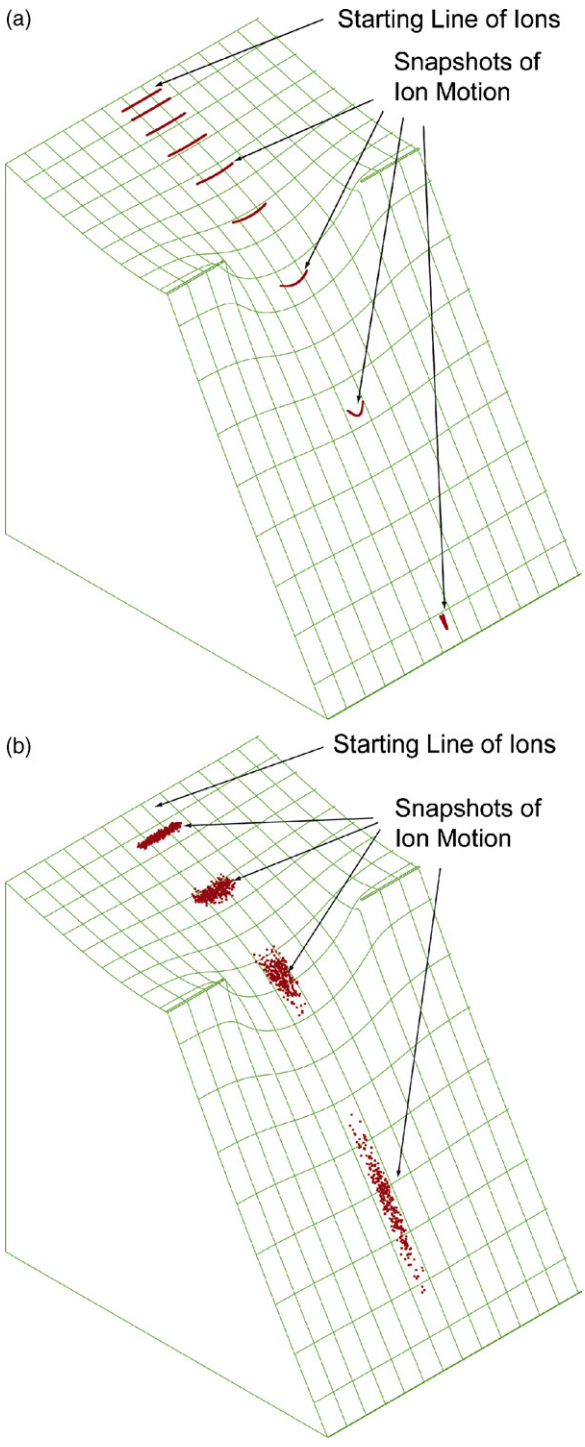

Fig. 2. Converging acceleration effects on ion cloud shape in (a) vacuum and (b) viscous conditions revealed using snapshots of ion motion. Ions introduced as a line source.

packet length) in the direction of the flight path. However, the ion packet at atmosphere pressure conditions becomes stretched into a serious loss of temporal focus (Fig. 2b). This spread along the direction of the flight path in the viscous regime is a result not only of diffusion, but also the increasing electrostatic field gradient that leads to differences in ion drift velocities. The variation in ion drift velocities is further exacerbated by the gradient variations within the curved field.

Fig. 3 illustrates the results of a diverging acceleration on ion motion in vacuum (Fig. 3a) and viscous (Fig. 3b) conditions. In vacuum, the ion packet accelerates and the terminal electrostatic field causes the ion packet line to diverge (i.e., increase in width along the direction normal to the flight path) with a slight distortion of the ion packet's line (Fig. 3a). The results of the simulation at atmospheric pressure (Fig. 3b) are dramatically

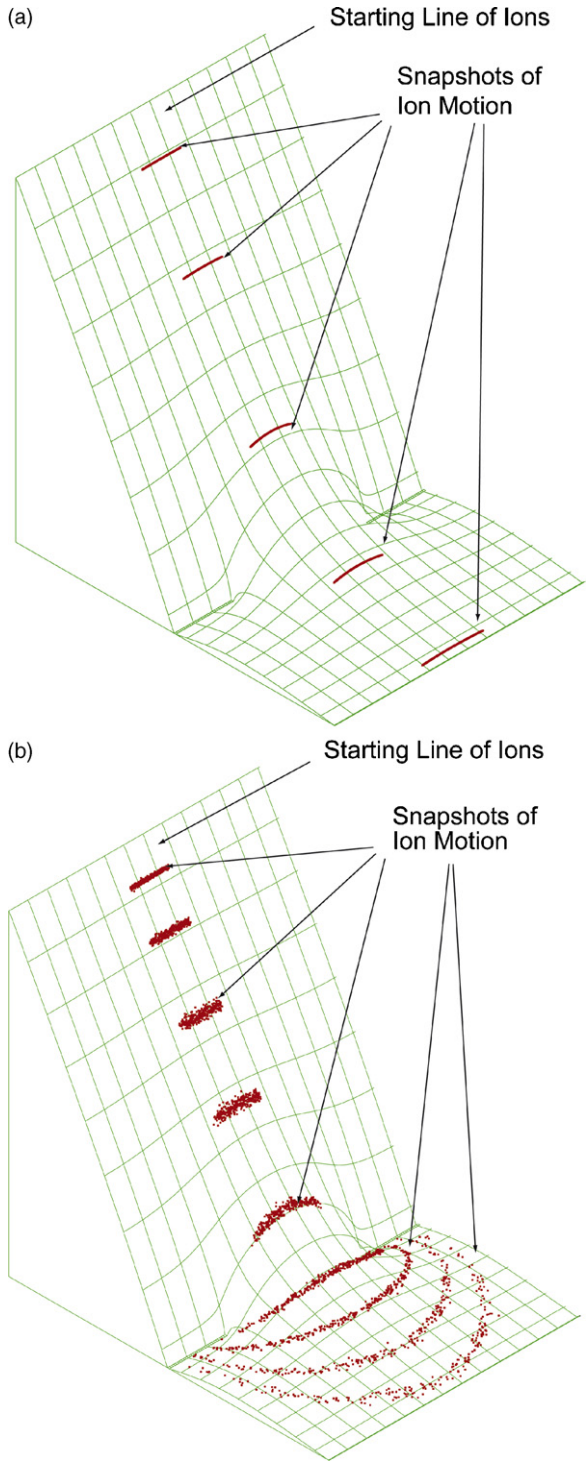

Fig. 3. Diverging acceleration effects on ion cloud shape in (a) vacuum and (b) viscous conditions illustrated using snapshots of ion motion. Ions introduced as a line source.

different from that in vacuum. Here, the ion packet diffuses and in the terminal field diverges, reminiscent of a wave spreading out through a slit. The ion trajectory effects in the viscous regime are again due to the lack of retained kinetic energy and diffusion. Because there are no collisions in the vacuum simulation, the retained kinetic energy of the ions tends to dominate their trajectories.

3.3. Grids with electrostatic gradients

Various forms of grids are often used for ion shutters or gates; therefore, modeling can provide insights into how grids affect ion motion both in vacuum and viscous environments, which is important for optimizing instrument performance. First, it is important to remember that if only one grid unit is used for SIMION modeling, the grid will act as an "ideal" grid. Hence, it is necessary to simulate a real grid by using more than one grid unit (e.g., four grid units in Figs. 4 and 5). Grid wires essentially work as small lenses; therefore, it is important to take into account the cumulative effect of these small lenses when designing instrumentation.

If the gradient is the same on both sides of a real grid, then the wires merely act to intercept and remove ions that happen to collide with them if the wire is in the ion's path. A grid can be used as an inflection point between two electrostatic gradients of different slopes, as shown in Fig. 4. If the initial gradient (entrance) slope the ions experience is less than the electrostatic gradient after the grid (exit), then a potential well or valley is developed between the wires of the grid (Fig. 4a), essentially creating a series of converging lenses. Because the potential wells are between the wires, more ions are guided through the grid, minimizing loss of ions. However, if the entrance gradient is greater than the exit gradient after the grid, then potential wells will form around the grid wires (Fig. 4b); thus, more ions will be funneled into and neutralized by collision with the wires. In vacuum, the survival rate of ions depends on their kinetic energy and the difference between the entrance and exit gradients, but in general, a higher survival rate is attained using gradient differentials similar to that shown in Fig. 4a than in Fig. 4b or if there is no gradient differential. However, grids will tend to defocus ion clouds slightly (similar to the refraction effects shown in Figs. 2 and 3) if the electrostatic gradients surrounding them are not equal in vacuum.

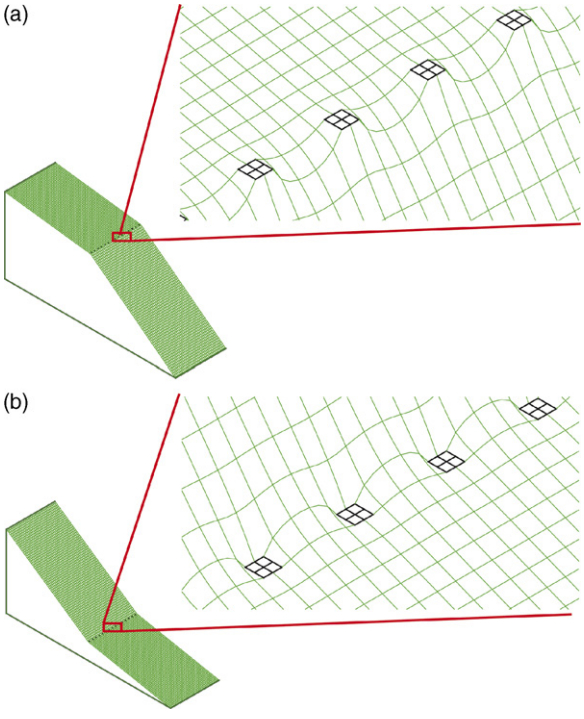

Fig. 4. Electrostatic potential around real wires occurs when the electrostatic gradient before the grid wires is (a) less than and (b) greater than the potential gradient after the grid. Insets show that potential wells exist between the wires when the slope of the initial electrostatic gradient is (a) less than the exit gradient, but around the wires when the slope is (b) greater than the final gradient.

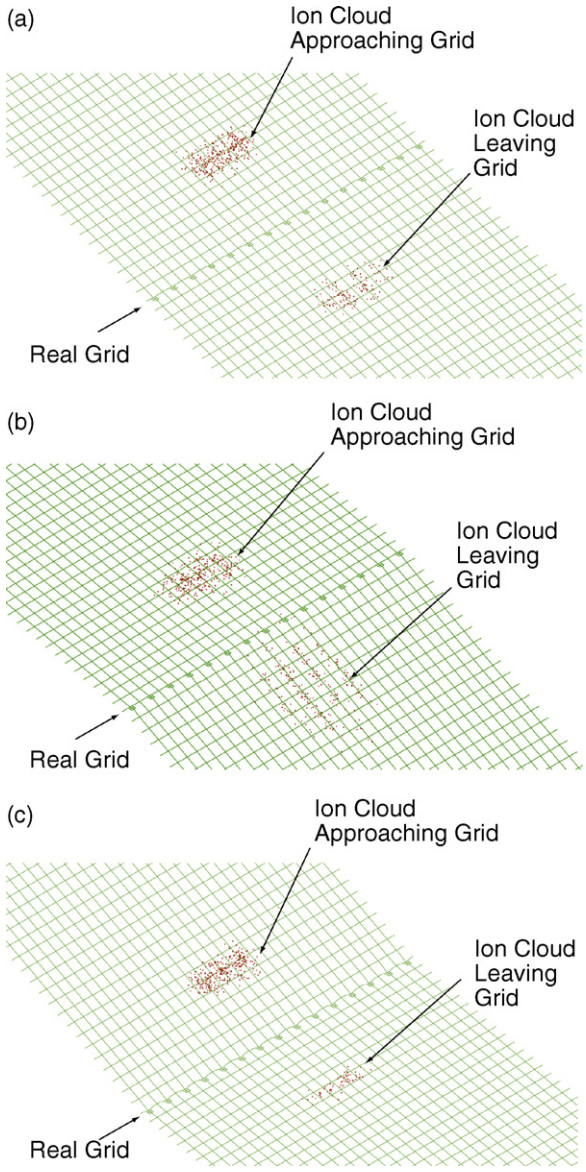

Fig. 5. Illustration of ion motion through real grids in viscous regime when the electrostatic gradient before the grid wires is (a) equal to, (b) less than, and (c) greater than the potential gradient after the grid.

As with real grids in vacuum, if the electrostatic gradients are the same on both sides of the grid in viscous media, the wires will merely intercept the ions if they are in the ion path. Fig. 5a shows an ion cloud before and after it passes through constant gradient grid transition at atmospheric pressure. While this reduces the number of ions, it does not significantly impact ion cloud dimensions (length or width).

However, if there is a gradient differential around the grid, then effects of real grids at atmospheric pressure can be quite different than in vacuum because the ions lose their kinetic energy to collisions, thus, leaving the ions more highly influenced by the localized electrostatic gradients. Fig. 5b demonstrates the condition where the exit gradient is greater than the entrance gradient. Again, the difference in the gradients acts to place the grid wires on ridges with electrostatic valleys (or wells) between the wires. Thus, most of the ions can pass through the grid without hitting a grid wire just as in vacuum. However, unlike the vacuum case, there is a dramatic increase in ion packet length because the ions do not retain any kinetic energy, similar to the converging refraction effect illustrated in Fig. 2b. This increase in ion cloud length is caused by two factors: the greater exit gradient acts to stretch the ion packet as ions first entering the gradient begin to move faster than those behind and the positive dimple fields around the grid wires retard ions that are being diverted around the wires to further contribute to the observed temporal defocusing.

Fig. 5c provides an example of a real grid where the exit gradient is less than the entrance gradient. Because this type of electrostatic gradient configuration causes the fields around the grid wires to form little wells, more ions are attracted to their death (i.e., neutralized) than the gradient setup in Fig. 5b. However, the exiting ion packet length is shorter than the entry packet length because the exit ion drift velocity is less than the entry ion velocity, which acts to pack the surviving ions closer together.

The best compromise for a viscous regime appears to be equalizing the electrostatic gradients on either side of the grid. Ion losses would be mostly limited to collisions with the grid wires, but the ion packet shape would be minimally impacted. This approach would be useful when considering gating or shutter strategies for releasing ions. If the goal is to retain most of the ions, this can be accomplished at the expense of increased ion packet length by using an exit gradient that is steeper than the entrance gradient. Alternatively, if the goal is to condense the ion packet length, this can be achieved by using an exit gradient that is shallower than the entrance gradient; however, the cost is a high rate of ion attrition due to increased collisions with the grid wires.

3.4. Magnetic field effects

It is insightful to use modeling to investigate the conditions necessary for a magnetic field to impact an ion's trajectory. Such insights can be useful for designing instruments that combine atmospheric sources with mass spectrometers, especially combining IMS with Fourier transform mass spectrometry (FTMS) instruments that use high magnetic fields [38].

If no external electrostatic fields are applied, an ion transversing a magnetic field in vacuum will orbit in a circle defined by its cyclotron radius and frequency [39]. The size of the cyclotron radius is a function of the strength of the magnetic field and the momentum of the ion, as defined by:

$$r_c = \frac{mv}{qB_0} \tag{1}$$

where r_c is the cyclotron radius, m the mass of the ion, q the charge on the ion, and v is the velocity perpendicular to the magnetic field (B_0). The frequency for the cyclotron motion (ω_c) is defined by:

$$\omega_c = \frac{qB_0}{m} \tag{2}$$

Thus, the effect of a 7 T magnetic field on a nitrogen molecular ion (N_2^+, m/z 28) results in a cyclotron radius of 1.9×10^{-5} m (assuming the thermal velocity (475 m/s) at 25 °C is perpendicular to B_0) and a cyclotron frequency of 3.8 MHz.

Fig. 6 illustrates the effect that varying magnetic fields have on ion trajectories at atmospheric pressure. In all magnetic field simulations, the first ion (blue) was flown with the magnetic field set to 0 T, while the second ion (red) was flown with the magnetic field turned on. Both simulations used a nitrogen molecular (N_2^+) ion flying within a bath gas of nitrogen (N_2) to eliminate any mass difference effects. A 7 T magnetic field, commonly used in FTMS [39], is a relatively strong magnetic field; however, there is no difference in the ion trajectories with or without the 7 T field present as shown in Fig. 6a. Even at 70 T, there is almost no difference in ion trajectories with the magnetic field present (data not shown). At 700 T a slight difference begins to occur (Fig. 6b), but it takes almost 7000 T for a magnetic field to have an appreciable affect on ion motion at atmospheric pressure (Fig. 6c).

A 7 T field has very little effect on ion diffusion trajectories at atmospheric pressure because the mean free path of an ion between collisions is only about 3.4×10^{-3} of the cyclotron radius for that ion. Thus, the ion will only have traveled ~0.05% along its cyclotron orbit before a collision occurs. Because the cord of a circle this short has almost no curvature, the ion's trajectory segment has almost no bending. Only when the magnetic field approaches 7000 T does the cyclotron radius become small enough to begin to overcome diffusion effects (Fig. 6c). At 7000 T, the ion in the magnetic field flies in little circular arcs because the ratio of the mean free path to cyclotron radius is 3.4, which means that the ion traverses approximately 50% of the cyclotron orbit between collisions, strongly modifying diffusion effects. The illustrations in Fig. 6 show magnetic effects for a single ion; however, it is useful to consider how the effects would be expressed for a swarm of ions. In a swarm of ions, each ion would have a random path so that the combined motion of the cloud of ions would show no significant change in expansion of the ion cloud for magnetic fields less than ~7000 T at atmospheric pressure. Only in extreme magnetic fields does the average distance traveled by the ions become compressed, leading to reduced diffusion (i.e., expansion) of the ion packet. A "rule-of-thumb" is that ions need to traverse a significant por-

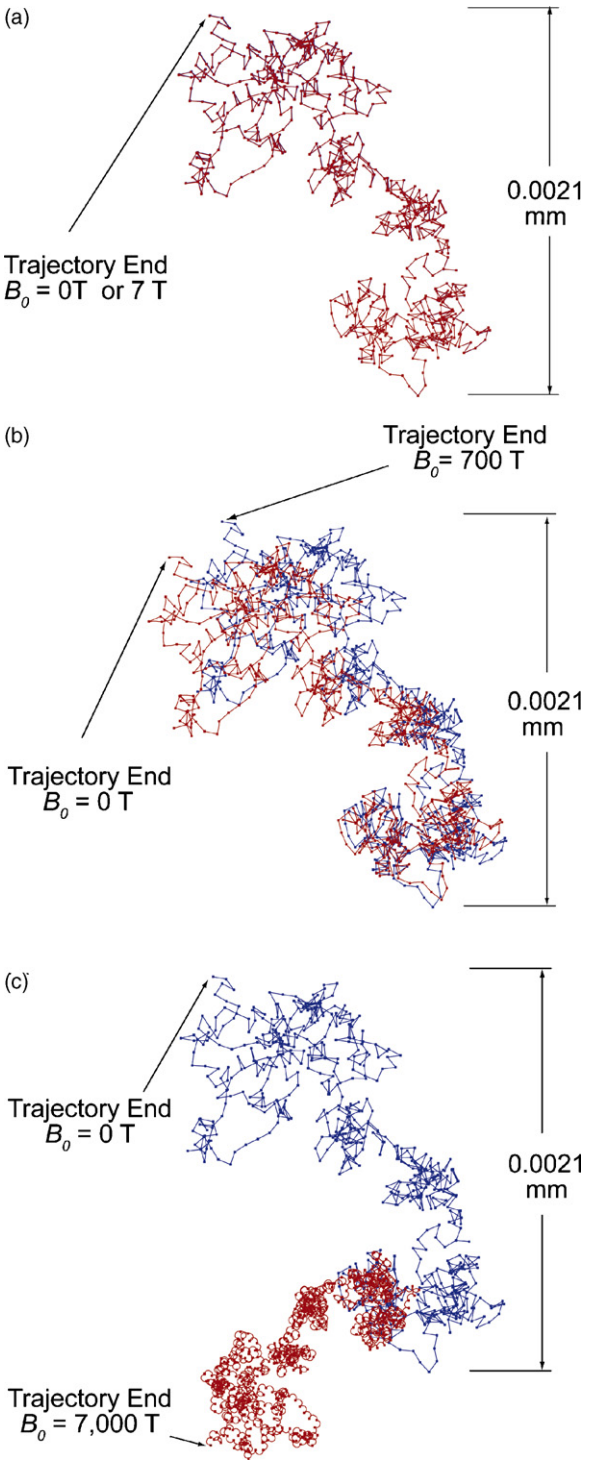

Fig. 6. Comparison of ion trajectories without and with a magnetic field present at atmospheric pressure. Nitrogen molecular ion (N_2^+) path in a nitrogen bath gas (N_2) with no magnetic field present (blue) is contrasted with the path in a magnetic field (red) for (a) 7 T, (b) 700 T, and (c) 7000 T. (For interpretation of the references to color in this figure legend, the reader is referred to the web version of the article.)

tion of their cyclotron radius (~50%) before a collision occurs for a magnetic field to begin to have a significant affect on diffusion. Alternatively stated, the cyclotron frequency must be approximately 50% of the collision rate before a magnetic field can induce an appreciable effect on ion cloud diffusion.

The same general result would occur if the time between collisions was increased (i.e., lower pressure) instead of increasing the intensity of the magnetic field because it is the ratio of the cyclotron orbit to mean free path (or cyclotron frequency to collision rate) that determines if the magnetic field will have an effect. Performing such a simulation with SIMION/SDS must be approached with caution because the diffusion calculation in SDS requires that there a sufficient number of collisions to decorrelate successive velocity vectors, otherwise SDS will over estimate diffusion effects.

Based on the extreme magnetic fields necessary to overcome diffusion, use of magnetic fields to control ion trajectories in viscous regimes is rather improbable at atmospheric pressure. However, magnetic fields combined with electrostatic fields can be used to influence ion trajectories for slightly reduced pressures as illustrated in Fig. 7. In the simulations used to create the illustrations in Fig. 7, the magnetic and electrostatic field

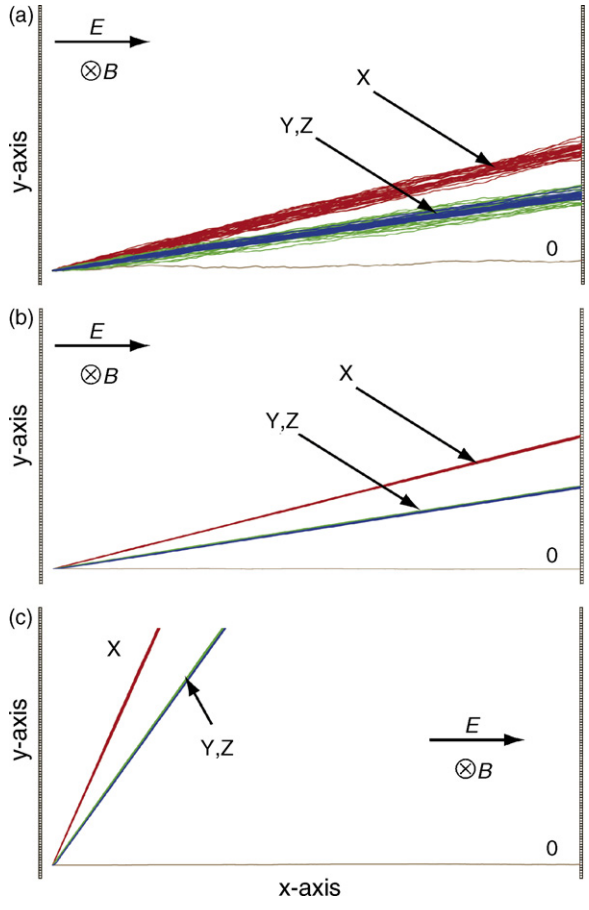

Fig. 7. Illustration of combined effect of magnetic and electrostatic fields on ion trajectories at less than atmospheric pressures: (a) 7 T magnetic field and 10^3 V electrostatic potential at pressure of 7.6 Torr, (b) 7 T magnetic field and 10^5 V electrostatic potential at pressure of 7.6 Torr or 70 T magnetic field and 10^5 V at 76 Torr, and (c) 70 T magnetic field and 10^5 V electrostatic potential at 7.6 Torr. Distance between electrodes set at 20 cm with electrostatic (E) and magnetic (B) field vectors orthogonal as indicated. Ion masses and K_0 values are: X (red) = 28 u, 3.08 $cm^2\ V^{-1}\ s^{-1}$; Y (green) = 90 u, 1.91 $cm^2\ V^{-1}\ s^{-1}$; and Z (blue) = 900 u, 1.91 $cm^2\ V^{-1}\ s^{-1}$. For reference, the 0 (tan) trace is that for a single ion without a magnetic field present. (For interpretation of the references to color in this figure legend, the reader is referred to the web version of the article.)

vectors are normal to each other. At atmospheric conditions (760 Torr), very little effect would be noticed for magnetic fields <7000 T and ions would merely follow the electrostatic gradient with the size of the ion cloud increasing due to diffusion. However, a minor reduction in pressure to 76 Torr would allow a 7 T magnetic field to slightly deflect the ions. Further decrease in pressure to 7.6 Torr allows for more deflection as shown in Fig. 7a. In Fig. 7a, a 7 T magnetic field imposed on a 50 V cm^{-1} electrostatic field is used to deflect three ion types. The mass and reduced mobility (K_0) of the X (red) ions were 28 u and 3.08 cm^2 V^{-1} s^{-1}, respectively. The Y (green) ions were assigned a mass and K_0 of 90 u and 1.91 cm^2 V^{-1} s^{-1}, respectively. For illustration purposes, the Z (blue) ions were assigned the same reduced mobility as the green ions, but defined as having a mass of 900 u. As expected for viscous regimes, the trajectories of the green and blue ions coincide because their motion is governed by size (i.e., mobility) and not mass. The trace labeled 0 (tan) is a typical trajectory of a single ion with no magnetic field present for reference. Any initial kinetic energy of the ions is essentially irrelevant under viscous conditions because it is rapidly dampened by collisions with the bath gas. For viscous conditions, increasing the electrostatic field by two orders of magnitude (from 10^3 to 10^5 V) does not change the deflection angles as shown in Fig. 7b. The electrostatic field has no apparent affect on the overall ion direction because the magnetic force is proportional to velocity × B_0; thus, the magnetic-induced velocity is proportional to the electrostatic-induced velocity, leading to a steady state that is independent of voltage gradient. While increasing the electrostatic gradient will not change the deflection angle, it does reduce the spread of the ion beam because the drift velocity will be faster, thus, reducing the time for diffusion (Fig. 7b). The angle of deflection can be altered either by changing the magnetic field or the pressure. For the same electrostatic gradient, the results in Fig. 7b can also be obtain using magnetic field of 70 T and a pressure of 76 Torr. Fig. 7c illustrates the deflection that a 70 T field can create at a lower pressure of 7.6 Torr. Thus, the angle of deflection is inversely proportional to the pressure and proportional to the magnetic field.

A simple equation estimating the angle of deflection can be derived from the differential equations that describe the force per unit charge on an ion in the x and y direction:

$$F(x) = m\frac{d^2x}{dt^2} = -\frac{1}{K}\frac{dx}{dt} - B\frac{dy}{dt} + E \tag{3}$$

$$F(y) = m\frac{d^2y}{dt^2} = -\frac{1}{K}\frac{dy}{dt} + B\frac{dx}{dt} \tag{4}$$

where E is the electrostatic gradient with units J m^{-1} C^{-1}, B the magnitude of the magnetic field in the negative z direction (consistent with Figs. 7 and 8) having units kg C^{-1} s^{-1}, K the local mobility with units C s kg^{-1}, m the mass per unit charge (kg C^{-1}) of the ion, and t is the time (s). If a steady state is assumed because ions quickly reach a terminal velocity in viscous conditions, then the acceleration terms in Eqs. (3) and (4) become zero resulting in Eqs. (5) and (6), respectively.

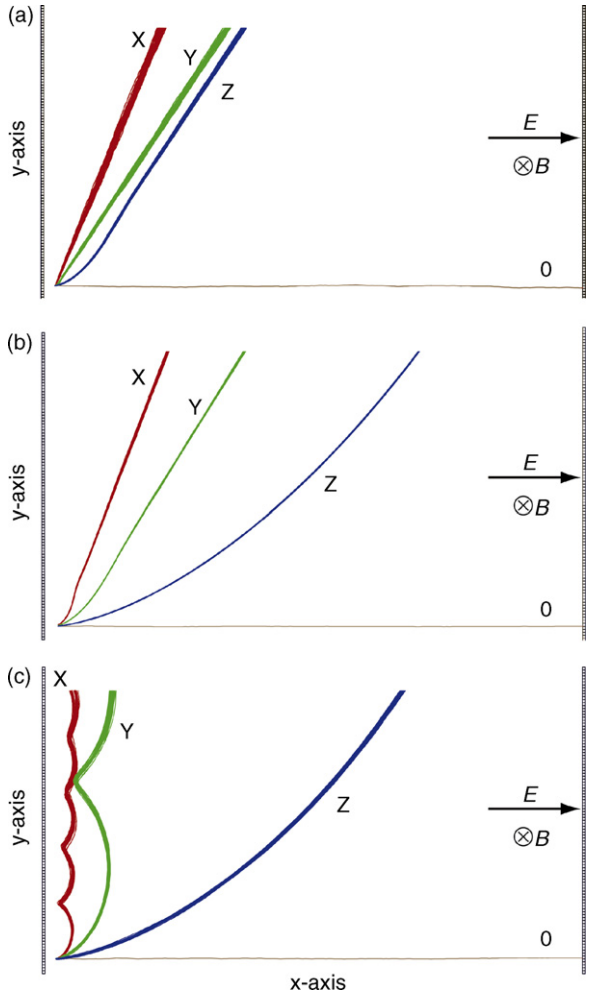

Fig. 8. Illustration of ion motion in quasi-viscous regime: (a) 7 T magnetic field and 10^4 V electrostatic potential at pressure of 0.76 Torr, (b) 7 T magnetic field and 10^5 V electrostatic potential at pressure of 0.76 Torr, and (c) 7 T magnetic field and 10^5 V electrostatic potential at 0.076 Torr. Distance between electrodes set at 20 cm with electrostatic (E) and magnetic (B) field vectors orthogonal as indicated. Ion masses and K_0 values are: X (red) = 28 u, 3.08 cm^2 V^{-1} s^{-1}; Y (green) = 90 u, 1.91 cm^2 V^{-1} s^{-1}; and Z (blue) = 900 u, 1.91 cm^2 V^{-1} s^{-1}. For reference, the 0 (tan) trace is that for a single ion without a magnetic field present. (For interpretation of the references to color in this figure legend, the reader is referred to the web version of the article.)

$$E = \frac{1}{K}v_x + Bv_y \tag{5}$$

$$Bv_x = \frac{1}{K}v_y \tag{6}$$

where v_x and v_y are the velocities (dx/dt and dy/dt) in the x and y directions, respectively. Solving by substitution for v_x and v_y:

$$v_y = E\frac{K^2B}{1 + K^2B^2} \tag{7}$$

$$v_x = E\frac{K}{1 + K^2B^2} \tag{8}$$

The ratio of v_y/v_y will give the tangent of the deflection angle (θ):

$$\tan\theta = \frac{v_y}{v_x} = KB \tag{9}$$

where K is related to the reduced mobility by:

$$K = K_0 \frac{P_0}{P}\frac{T}{T_0} \tag{10}$$

thus, the deflection angle for a given ion can by estimated by:

$$\theta = \tan^{-1}\ BK_0 \frac{P_0}{P}\frac{T}{T_0} \tag{11}$$

as a solution for a single elementary charge on the particle. The reason unitary charged was assumed is that the charge (q) is embedded in K. In most equations in physics and chemistry, q is a separate entity (e.g., qE to define force). Incorporation of q into K can cause confusion and consternation. As a result, when the charge is doubled, K is doubled, which will double the slope.

If the pressure is reduced to 0.76 Torr for a magnetic field of 7 T and an electrostatic gradient of 500 V cm^{-1} as shown in Fig. 8a, a separation of the Y and Z ions (green and blue, respectively) with identical K_0 values, but different masses, is observed because the mean free path between collisions is large enough that inertial effects come into play. The separation of the ions based on mass reveals that this pressure regime is only quasi-viscous. At this point, the calculations begin to become dubious. While the observed effects may be real, the actual value of the parameters (i.e., pressure, electrostatic gradient, magnetic field strength) that these effects would occur at in reality may not match that predicted by the simulation. Because of inertial effects, the electrostatic field gradient will also affect ion trajectories as shown in Fig. 8b, where the electrostatic potential has been increase by an order of magnitude (from 10^4 to 10^5 V) compared to Fig. 8a. Fig. 8c shows the ion trajectories at a pressure of 0.076 Torr for the same conditions as Fig. 8b. The semi-loops in the ion motion result from the superposition of the cyclotron motion on the ion trajectories. The width of the ion beams in Fig. 8c is slightly wider than in Fig. 8b, even though the pressure is lower, suggesting that the simulations may have exceeded the diffusion calculation limits. Indeed, lowering the pressure or increasing either the magnetic or electrostatic fields results in wide ion beams because the velocities are no longer decorrelated, leading to an over estimation of diffusion. Simulations in the quasi-viscous regime must be viewed with caution because results using SIMION/SDS under these conditions have not been benchmarked against experimental data as they have for viscous conditions [31].

3.5. Charge repulsion effects

Charge repulsion effects were not included in the simulations presented. Although limited charge repulsion modeling is available in SIMION, the calculations add an n-factorial load on the computations. Inclusion of Coulombic repulsion should be considered in the final modeling of viscous instruments by SIMION/SDS because charge repulsion is more problematic when ions are moving slowly, which is true throughout an instrument operating at higher pressures close to or at atmosphere. Charge repulsion reveals itself as an increase in the effective diffusion as the ions repel each other. In vacuum instruments, ions generated at a source are moving slowly, but then are normally accelerated to high velocity throughout the rest of the instrument. Therefore, charge repulsion modeling in vacuum is most relevant for exploring issues around ionization sources.

4. Conclusions

Simulations of ion motions illuminate differences between vacuum and viscous environments that are important for mass spectrometry and ion mobility instruments. In vacuum, kinetic energy plays a dominant role in ion trajectories; however, in viscous regimes collisions quickly dampen ion kinetic energy effects. Thus, in viscous environments without electrostatic gradients, ion motion will be limited to diffusion. Unlike in vacuum, viscous refractive effects can only be obtained in accelerating electrostatic gradients. For viscous atmospheres, converging refractive gradients decrease the ion cloud radially, but disperse the ions more longitudinally. Conversely, diverging gradients in viscous regimes decrease the longitudinal spreading of the ions, but increase their radial distribution. Grids generally have a far more significant impact in viscous environments than in vacuum due to refraction and scavenging by the wires. Magnetic-induced effects with practical magnetic fields at atmospheric pressure on Earth are negligible; however, reduction in pressure by one or two orders of magnitude does provide an opportunity to influence ion trajectories with magnetic fields. Caution must be taken when simulating ion motion in the transition between viscous and vacuum pressure regions because SDS diffusion calculations require that ion velocities are decorrelated between time steps. Thus, when using simulations, the admonition to "always be suspicious" should be kept in mind [34].

Acknowledgement

The authors gratefully acknowledge support from the United States Department of Energy under DOE/NE Idaho Operations Office Contract DE-AC07-05ID14517.

References

[1] M.W. Forbes, M. Sharifi, T. Croley, Z. Lausevic, R.E. March, J. Mass Spectrom. 34 (1999) 1219.
[2] D.A. Dahl, Int. J. Mass Spectrom. 200 (2000) 3.
[3] D.A. Dahl, J.E. Delmore, A.D. Appelhans, Rev. Sci. Instrum. 61 (1990) 607.
[4] American Mass Spectrometry Society, http://www.asms.org/Default.aspx?tabid=127, accessed April 19, 2007.
[5] P. Benetti, G. Fossati, M. Rossella, A. Tomaselli, F. Sigon, Inst. Phys. Conf. Ser. (1991) 373.
[6] S. Biri, A. Bader, J. Palinkas, Rev. Sci. Instrum. 67 (1996) 1483.
[7] G.S. Jackson, J.D. Canterbury, S.H. Guan, A.G. Marshall, J. Am. Soc. Mass Spectrom. 8 (1997) 283.
[8] S. Prusa, J. Zlamal, T. Sikola, Nucl. Instrum. Methods Phys. Res. Sect. B: Beam Interact. Mater. Atoms 137 (1998) 822.
[9] G.A. Salazar, T. Masujima, J. Am. Soc. Mass Spectrom. 18 (2007) 413.

[10] O. Sise, M. Ulu, M. Dogan, Radiat. Phys. Chem. 76 (2007) 593.
[11] M. Ulu, O. Sise, M. Dogan, Radiat. Phys. Chem. 76 (2007) 636.
[12] J. Zhang, C.G. Enke, Eur. J. Mass Spectrom. 6 (2000) 515.
[13] J. Zhang, B.D. Gardner, C.G. Enke, J. Am. Soc. Mass Spectrom. 11 (2000) 765.
[14] D.E. Austin, D. Cruz, M.G. Blain, J. Am. Soc. Mass Spectrom. 17 (2006) 430.
[15] J. Lorincik, K. Franzreb, P. Williams, Appl. Surf. Sci. 231/232 (2004) 921.
[16] C. Ma, H.W. Lee, D.M. Lubman, Appl. Spectrosc. 46 (1992) 1769.
[17] V. Palonen, P. Tikkanen, J. Keinonen, Nucl. Instrum. Methods Phys. Res. Sect. B: Beam Interact. Mater. Atoms 223–224 (2004) 227.
[18] M. Rachev, R. Srama, A. Srowig, E. Grun, Nucl. Instrum. Methods Phys. Res. Sect. A: Accel. Spectrom. Dect. Assoc. Equip. 535 (2004) 162.
[19] W.J. Sun, J.C. May, D.H. Russell, Int. J. Mass Spectrom. 259 (2007) 79.
[20] I.V. Veryovkin, W.F. Calaway, M.J. Pellin, Nucl. Instrum. Methods Phys. Res. Sect. A: Accel. Spectrom. Dect. Assoc. Equip. 519 (2004) 363.
[21] V. Grill, H. Drexel, W. Sailer, M. Lezius, T.D. Mark, J. Mass Spectrom. 36 (2001) 151.
[22] D.Q. Hu, K.T. Leung, Rev. Sci. Instrum. 66 (1995) 2865.
[23] P.Y. Kwan, S. Fung, C.D. Beling, Appl. Surf. Sci. 194 (2002) 32.
[24] A.L. Victor, T.H. Zurbuchen, A.D. Gallimore, Rev. Sci. Instrum. 77 (2006).
[25] T.J.M. Zouros, O. Sise, M. Ulu, M. Dogan, Meas. Sci. Technol. 17 (2006) N81.
[26] P.C. Arnold, D.G. Bills, M.D. Borenstein, S.C. Borichevsky, J. Vac. Sci. Technol. A: Vac. Surf. Films 12 (1994) 580.
[27] G. Balla, A.D. Koutselos, J. Chem. Phys. 119 (2003) 11374.
[28] A.D. Koutselos, J. Phys. B: At. Mol. Opt. Phys. 32 (1999) 1225.
[29] J.R. Scott, P.L. Tremblay, Rev. Sci. Instrum. 78 (2007) 035110.
[30] O. Soppart, J.I. Baumbach, Meas. Sci. Technol. 11 (2000) 1473.
[31] A.D. Appelhans, D.A. Dahl, Int. J. Mass Spectrom. 244 (2005) 1.
[32] Handbook of Chemistry and Physics, 64th ed., CRC, Boca Raton, 1984.
[33] J.W. Moore, R.G. Pearson, Kinetics and Mechanism, 3rd ed., John Wiley & Sons, New York, 1981.
[34] D.A. Dahl, SIMION 3D Version 7.0 User's Manual. Idaho National Engineering and Environmental Laboratory, Bechtel BWXT Idaho, LLC, Idaho Falls, ID, 2000.
[35] C.M. Lock, E.W. Dyer, Rapid Commun. Mass Spectrom. 13 (1999) 422.
[36] G.A. Eiceman, Z. Karpas, Ion Mobility Spectrometry, 2nd ed., CRC Press, Boca Raton, 2005.
[37] O. Sise, M. Ulu, M. Dogan, Nucl. Instrum. Methods Phys. Res. Sect. A: Accel. Spectrom. Dect. Assoc. Equip. 554 (2005) 114.
[38] B.K. Bluhm, K.J. Gillig, D.H. Russell, Rev. Sci. Instrum. 71 (2000) 4078.
[39] A.G. Marshall, F.R. Verdun, Fourier Transforms in NMR, Optical, and Mass Spectrometry: A User's Handbook, Elsevier, New York, 1990.